Chaos Behavior of Voltage Control Oscillator based on Colpitts Oscillator

F. Setoudeh , M. Dousti

Department of Electrical and Computer Engineering, Science and Research branch, Islamic Azad University, Tehran, Iran.
E-mails: f.setoudeh@srbiau.ac.ir, m_dousti@srbiau.ac.ir

Abstract: A Voltage-Control Oscillator (VCO) based on Colpitts oscillator is analyzed from a chaos theory viewpoint. Sensitivity to initial conditions is studied by considering a nonlinear model of the system, and also a new chaos analysis methodology based on the energy distribution using the Discrete Wavelet Transform (DWT) is presented, Then using Advance Designs System (ADS) software, implementation of chaotic VCO based on Colpitts oscillator using RF-CMOS 0.18 μm technology is considered. Simulation results are provided to show the main points of the paper.

Keywords: Chaos, Colpitts oscillator, Voltage control oscillator (VCO), Stability, Lyapunov exponent.

1. INTRODUCTION

Chaos is widely available in engineering and the natural systems. Chaos phenomenon is completely deterministic and specific to nonlinear systems. In fact, chaos theory is a branch of mathematics and physics related to systems that their dynamic represents a very sensitive behavior to changes in the initial values so that their future behavior is not predictable. Nowadays, there are examples of potential benefits of the chaotic behavior that make a lot of engineers and researchers attend it. For instance, it can be referred to the application of chaos in communication systems, information coding, etc. (Kennedy, 1994; Lie and Yuan, 2000; Knop and Huseh, 2001; Shi and Tong, 2010); however, in some systems, chaos is considered as a nuisance factor, and if possible, in designing, it is removed from the system. This is why, in this system, the first step is to identify chaos. Chaotic dynamics occur based on certain rules that are seemingly random. In contrast, for dynamics random made that process no structure other than its probability distribution cannot be achieved. From the observation of time series obtained from a process, detecting a non-linear and chaotic nature is almost impossible. The study on nonlinear dynamic systems is an important topic for research scholars. Behavior of complex systems, clearly this phenomenon is chaos.

In recent years, many researchers have attempted analyzing the chaotic behavior of electronic circuits because a simple electronic component can be easily implemented on the circuits, also in this circuit, the control guidelines are easily accessible by physical guidelines such as voltage, current, resistance occurs. The second reasons, according to the researchers, these circuits are very much applicable in practicable engineering systems such as electronic communication systems. One of these electronic circuits occurs in that chaos is sinusoidal oscillator circuits. Oscillator circuits have many applications in systems such as swing transceiver circuits, communication systems, so they can be considered one important component of electronic systems. Colpitts oscillator is used to produce a periodic sinusoids signal under some specific conditions in microwave

Frequency. In recent years, many researchers have attempted analyzing the chaotic behavior of chaotic oscillator namely: Kennedy showed the chaos in the Colpitts oscillator, he proposed its applications in the encryption and modulation methods applied to the communication systems (Kennedy, 1994). Lie et al. showed the existence of bi-stable behavior and chaotic regions in dependence on the driving frequency (Lie and Yuan, 2000). Knop et al. provided the bifurcation diagrams, fixed-pointed diagrams and phase diagrams for two damping constants and found the typical period-doubling route to chaos (Knop and Huseh, 2001). Shi et al. proposed the stability analysis and a necessary condition to generate chaos in 3D chaotic oscillator (Shi and Tong, 2010). A. Tama proposed a simple 4D hyper chaotic oscillator (Tama et al., 1996). Kengne et al. worked on the dynamical properties and the chaos synchronization of the improved Colpitts oscillators as well (Kengne et al., 2011).

Effa et al. proposed a smooth mathematical model to investigate the dynamics and synchronization behavior of the improved Colpitts oscillator (Effa et al., 2009; Effa et al., 2009). Trueba, et al. propose that the effect of nonlinear dissipation on certain nonlinear oscillators (Zhu et al., 2011). (Volkovskii, et al., 2005) proposes a new spread spectrum communication system utilizing chaotic frequency modulation of sinusoidal signals. They study the dynamics of the synchronization process, stability of the PLL system, and evaluate the bit-error-rate performance of this chaos-based communication system.

In this paper, an integrated voltage control and the chaos phenomenon is analyzed accurately in this circuit considering a nonlinear model of the transistor. The numerical simulation has been done by Advanced Design System (ADS) and MATLAB. The electronic control of the oscillator is considered as a very efficient tool for generating many chaotic signals in a short settling time. The main outlined of this paper is as follows: Section 2 describes the chaotic Colpitts oscillator, section 3 describes analysis of VCO based on Colpitts oscillator, section 4 proposed dynamical analytical of the chaotic VCO system, including dissipativity, Lyapunov exponents. Section 5 proposed the simulation results, section 6 proposed power density spectrum analysis and then a methodology based on the energy distribution is presented using the Discrete Wavelet Transform (DWT) for chaos analysis are presented in Section 7. Finally Section 8 concludes the paper.

2. CHAOTIC COLPITTS OSCILLATOR PRELIMINARIES

Colpitts oscillator is another type of LC oscillator design. In many ways, the Colpitts oscillator is the exact opposite of the Hartley oscillator. Just like the Hartley oscillator, the tuned tank circuit consists of a LC resonance sub-circuit connected between the collector and the base of a single stage transistor amplifier producing a sinusoidal output waveform. The Colpitts oscillator uses a single stage bipolar transistor amplifier as the gain element which produces a sinusoidal output. The single ended chaotic Colpitts oscillator is shown in Figure 1. The Colpitts oscillator is a combination of a transistor amplifier consisting of a single bipolar junction transistor (BJT), and a LC circuit which has been used to feedback the output signal as it is shown in Figure 1. The fundamental oscillation frequency is given by:

$$f=\frac{1}{2\pi\sqrt{L_1\frac{C_1C_2}{C_1+C_2}}} \tag{1}$$

Presence of a positive Lyapunov Exponent (LE) confirms the occurrence chaotic behavior in the Colpitts oscillator.

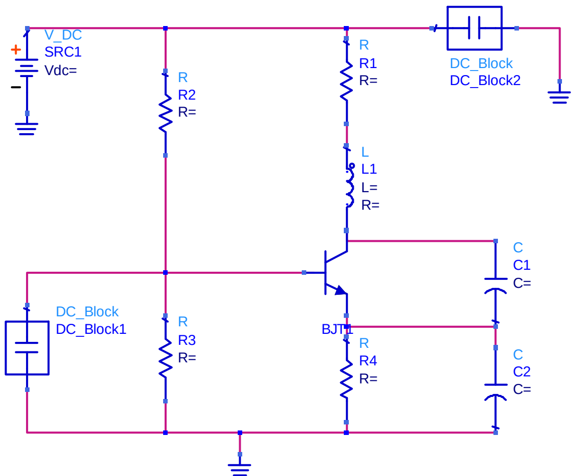

Fig. 1. Circuit Layout of the single ended chaos Colpitts oscillator.

Dynamic behavior of above oscillator describe by following equation:

$$\begin{bmatrix}\dot{x}\\ \dot{y}\\ \dot{z}\end{bmatrix}=\begin{bmatrix}\frac{g}{Q(1-K)}\left[-n(y)+z\right]\\ \frac{g}{QK}z\\ \frac{-QK(1-K)}{g}\left[x+y\right]-\frac{1}{Q}z\end{bmatrix},\quad n(y)=\exp(-y)-1 \tag{2}$$

where: $x=V_{C_1},\quad y=V_{C_2},\quad z=V_{C_3},\quad g=\frac{I_0L}{V_TR(C_1+C_2)},$

$$K=\frac{C_2}{C_1+C_2},\quad Q=\frac{\omega_0L}{R},\quad \omega_0=\frac{1}{\sqrt{L\frac{C_1C_2}{C_1+C_2}}}$$

The circuit parameters are selected as:

$g=2.8009,\quad Q=1.7678,\quad K=0.5.$

The equilibrium point of the system (2) is:

$(x_e=0,\quad y_e=0,\ z_e=0).$

The Jacobean matrix near the equilibrium point is given by:

$$J=\begin{bmatrix}0 & \frac{g}{Q(1-K)}a & \frac{g}{Q(1-K)}\\ 0 & -\frac{g}{QK}(1-a) & \frac{g}{QK}\\ \frac{-QK(1-K)}{g} & \frac{-QK(1-K)}{g} & -\frac{1}{Q}\end{bmatrix} \tag{3}$$

The eigenvalues of the equilibrium state can be calculated as:

$|\lambda_i I-J|=0$

The eigenvalues of the equilibrium state (0, 0, and 0) can be written as:

$$\begin{cases}\lambda_1=-1.8545\\ \lambda_{2,3}=0.6381\pm 1.4024i\end{cases} \tag{4}$$

Thus, an unstable saddle characterized them focus. The circuit performs chaotic behaviors. Chaotic behavior of chaotic Colpitts has been shown in Figures 2 and 3. Transient chaotic attractor and 3D chaotic attractor under different condition are shown in Figures 2 and 3.

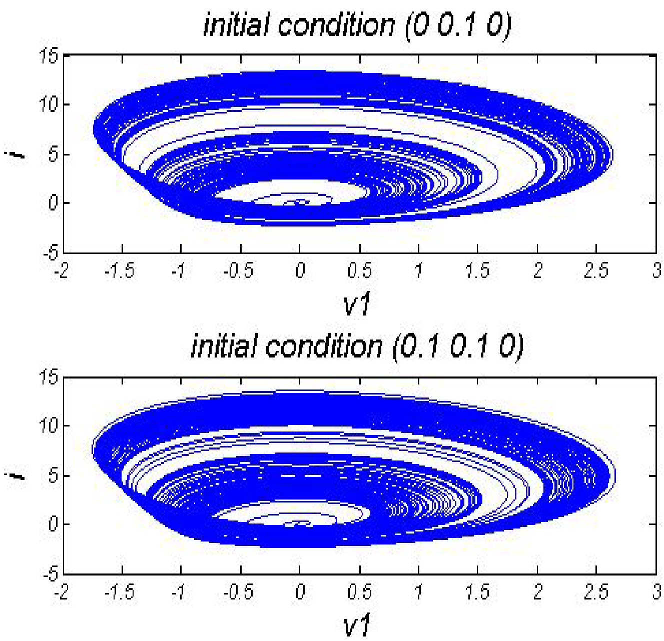

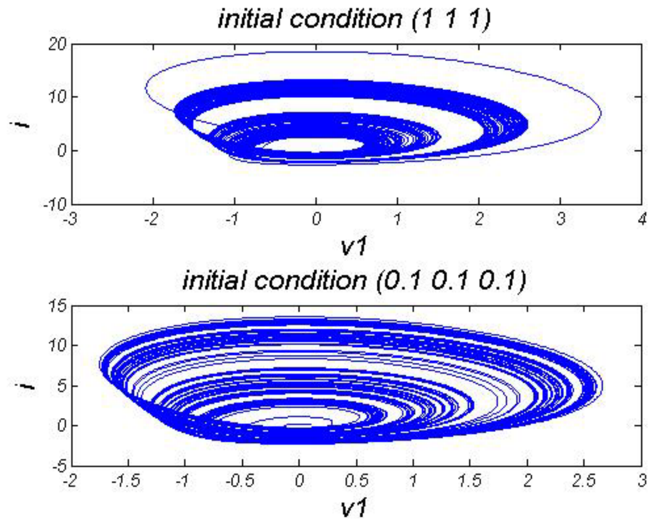

Fig. 2. Chaotic attractor of Colpitts oscillator.

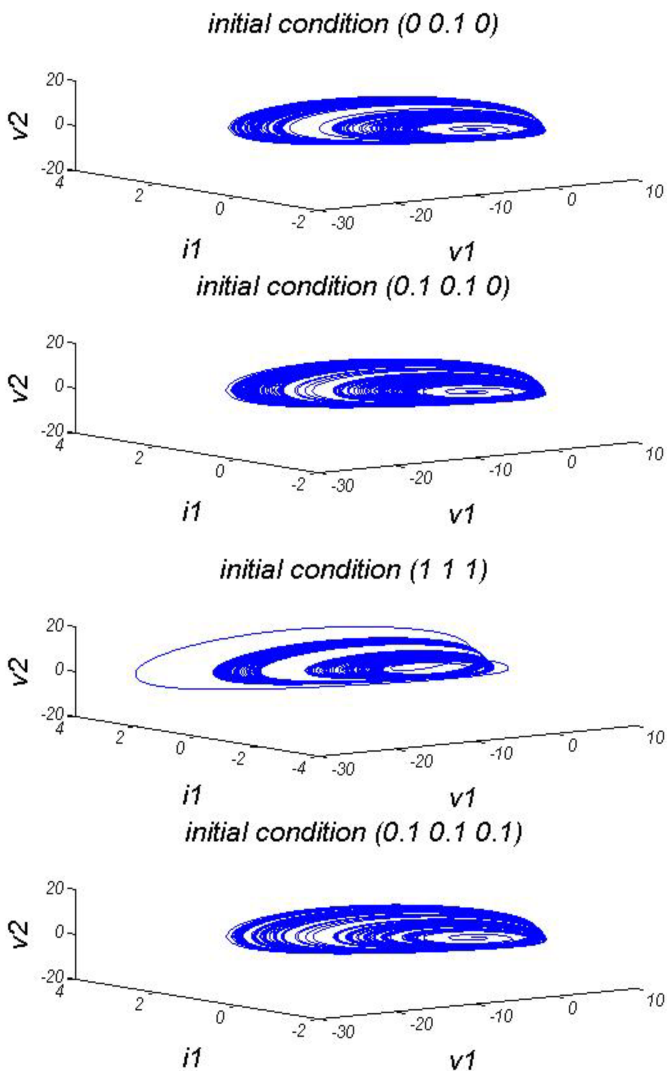

Fig. 3. 3D. chaotic attractor of Colpitts oscillator.

Figure 4 shows an ADS implementation of improved Colpitts oscillator. The difference between the standard circuit schematic diagram of the Colpitts oscillator and the improved version is the presence of inductor L_5 in series with resistor R_7 in the base circuit.

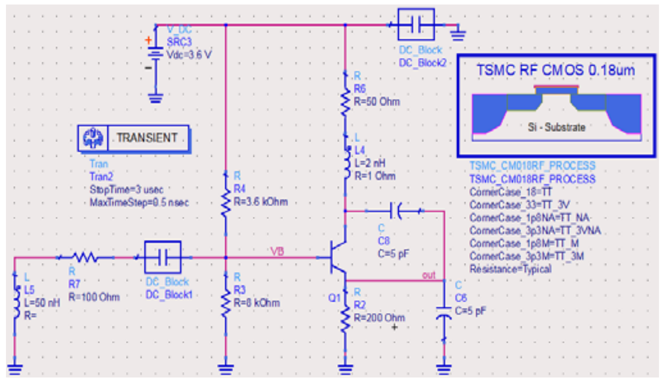

Fig. 4. the schematic diagram of the improved Colpitts oscillator in ADS.

Figure 5 shows the simulation results.

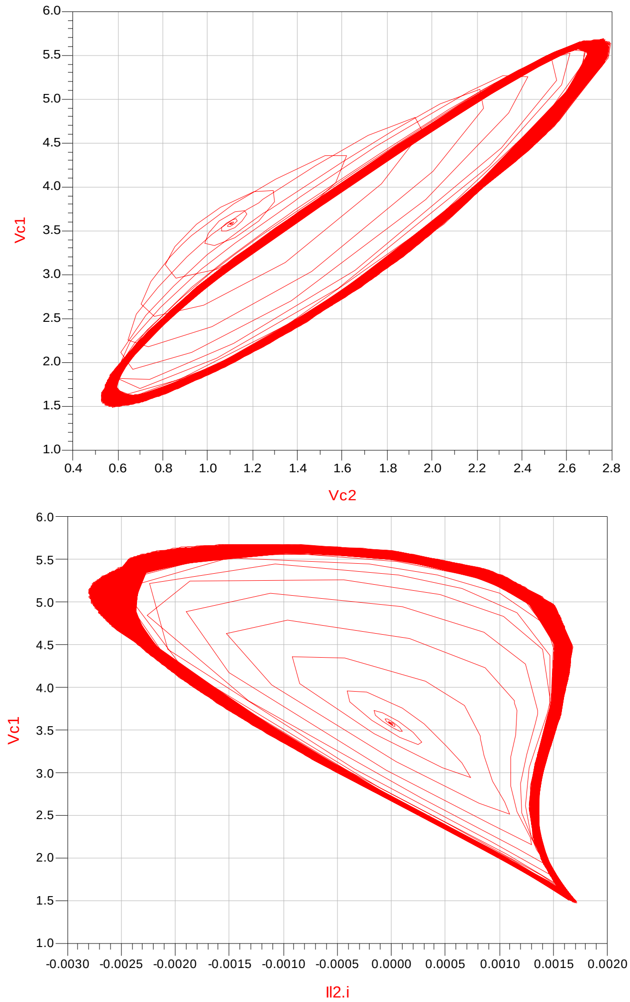

Fig. 5. Simulation results of improved Colpitts oscillator.

3. ANALYSIS OF THE CHAOTIC VCO

Figure 6 shows an ADS implementation of VCO.

Using the Kirchhoff rules, the dynamic equations describing the circuit are as follows:

$$\begin{cases} C_1 \dfrac{dV_{C_1}}{dt} = \dfrac{V_{cc} - V_{C_1} - V_{C_2}}{R_2} - \dfrac{f(V_{C_1})}{\beta} - I_L \\ C_2 \dfrac{dV_{C_2}}{dt} = \dfrac{V_{cc} - V_{C_1} - V_{C_2}}{R_2} + f(V_{C_1})(1 - \dfrac{1}{\beta}) - I_L - \dfrac{V_{C_2}}{R_3} \\ L \dfrac{dI_L}{dt} = V_{C_1} + V_{C_2} + V_{C_4} - R_4 I_L \\ C_3 \dfrac{dV_{C_3}}{dt} = -I_L \\ C_4 \dfrac{dV_{C_4}}{dt} = \dfrac{V_B - V_{C_4}}{R_b} - I_L + I_s \end{cases} \tag{5}$$

where:

$$f(V_{C_1}) = I_s(\exp\left(\frac{V_{C_1}}{V_T}\right) - 1)$$

Obviously, the Jacobean matrix is:

$$J = \begin{bmatrix} \dfrac{1}{C_1}(\dfrac{-1}{R_2} - \dfrac{f_1(V_{C_1})}{\beta V_T}) & \dfrac{1}{C_1}(\dfrac{-1}{R_2}) & \dfrac{-1}{C_1} & 0 & 0 \\ \dfrac{1}{C_2}(\dfrac{-1}{R_2} + \dfrac{f_1(V_{C_1})(1-\dfrac{1}{\beta})}{V_T}) & \dfrac{1}{C_2}(\dfrac{-1}{R_2} - \dfrac{1}{R_3}) & \dfrac{-1}{C_2} & 0 & 0 \\ \dfrac{1}{L} & \dfrac{1}{L} & \dfrac{-R}{L} & \dfrac{1}{L} & \dfrac{-1}{L} \\ 0 & 0 & \dfrac{-1}{C_3} & 0 & 0 \\ 0 & 0 & \dfrac{1}{C_4} & 0 & \dfrac{-1}{R_b C_4} \end{bmatrix} \tag{6}$$

where: $f_1\left(V_{C_1}\right) = I_s \exp\left(\dfrac{V_{C_1}}{V_T}\right)$

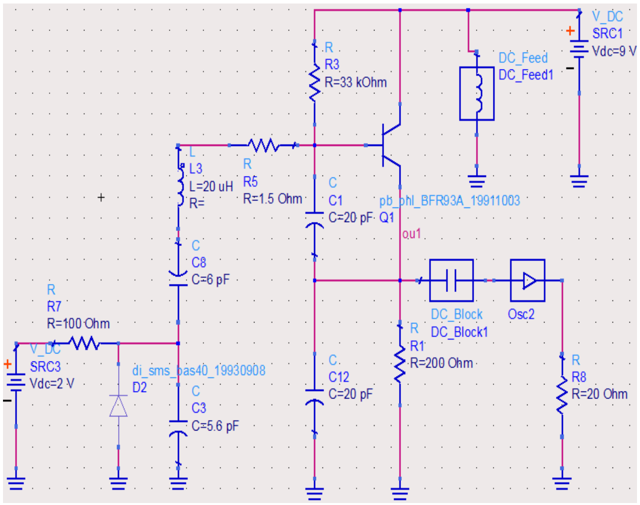

Fig. 6. Circuit layout of chaotic voltage control oscillators.

So, the dimensionless equilibrium point equations of the system (5) are:

$$\begin{cases} \dfrac{V_{cc} - V_{C_1} - V_{C_2}}{R_2} - \dfrac{f\left(V_{C_1}\right)}{\beta} = 0 \\ \dfrac{V_{cc} - V_{C_1} - V_{C_2}}{R_2} + f\left(V_{C_1}\right)\left(1 - \dfrac{1}{\beta}\right) - \dfrac{V_{C_2}}{R_3} = 0 \\ V_{C_1} + V_{C_2} + V_{C_4} = 0 \\ \dfrac{V_B - V_{C_4}}{R_b} + I_s = 0 \\ I_L = 0 \end{cases} \tag{7}$$

where:

$V_{cc} = 9V, V_B = 1.2V, R_2 = 3.6k\Omega, R_3 = 300\Omega, R_b = 1k\Omega$

Accordingly, the matrix (6) is analyzed to investigate the stability of the equilibrium points. So the system (5) about the equilibrium point is unstable because one of the Eigen values of system (5) is positive.

4. DYNAMICAL BEHAVIORS OF THE SYSTEM

In this section, the dynamical behaviors of the proposed chaotic VCO proposed with the aid of conventional dynamic analytical approaches, including dissipativity, Lyapunov exponents.

4.1. Dissipativity

Consider chaotic dynamical system (5), if in a system phase space we consider some part of level S, and if $S(t)$ level changes into $S(t + dt)$, so the V volume will change as follow:

$$\dot{V} = \frac{V(t+dt) - V(t)}{dt} = \int f.n\,dA = \int \nabla f\, dV \tag{8}$$

where:

$$\nabla f = \frac{\partial \dot{x}_1}{\partial x_1} + \frac{\partial \dot{x}_2}{\partial x_2} + \frac{\partial \dot{x}_3}{\partial x_3} + \frac{\partial \dot{x}_4}{\partial x_4} + \frac{\partial \dot{x}_5}{\partial x_5} \tag{9}$$

where:

$$\left(x_1 x_2 x_3 x_4 x_5\right)^T = \left(V_{C_1} V_{C_2} I_L V_{C_3} V_{C_4}\right)^T$$

Then, the divergence of the vector field is negative.

$$\nabla f = \frac{1}{C_1}\left(\frac{-1}{R_2} - \frac{f_1\left(V_{C_1}\right)}{\beta V_T}\right) + \frac{1}{C_1}\left(\frac{-1}{R_2} - \frac{1}{R_3}\right) - \frac{R}{L} - \frac{1}{R_b C_4} < 0 \tag{10}$$

So the system is always dissipative.
As a result, for the V volume, we have:

$$V(t) = V_0\, e^{\left(\frac{1}{C_1}\left(\frac{-1}{R_2} - \frac{f_1\left(V_{C_1}\right)}{\beta V_T}\right) + \frac{1}{C_1}\left(\frac{-1}{R_2} - \frac{1}{R_3}\right) - \frac{R}{L} - \frac{1}{R_b C_4}\right)t} \tag{11}$$

That is, the flow contracted a volume element V_0 into a volume element $V(t)$ at time t. This means that each volume containing the system orbit shrinks to zero as $t \to 0$. Therefore, all the trajectories of the system will be eventually confined to a subset that has been zeroing volume, and the asymptotic motion will settle onto an attractor of the system.

4.2. Lyapunov Exponents

One powerful tool for detecting chaos is Lyapunov exponent (LE). LE yield numerical criteria of the quantity of chaotic behavior of a system. Using the LE, sensitivity of a mapping to initial conditions can be considered (Tama et al., 1996). If the sign of LE is positive, the system is chaotic, and if it is negative, it is not chaotic (Tama et al., 1996; Kengne et al., 2011). Various ways have been proposed for calculating the LE so far; one of these ways is to calculate the LE using time series (Effa et al., 2009). However, the LE is highly sensitive to noise, so the use of LE in noisy environments is not a good criterion for detecting chaos (Effa et al., 2009; Zhu, 2011).

In order to analyze the chaos more accurately and show sensitivity to the initial conditions, LE of the system is calculated. Before computing the LE, the time scales for the first two circuits are scaled to the order of seconds by: $= \sqrt{L\frac{C_1C_2}{C_1+C_2}}$. The existence of a positive LE indicates chaos in this circuit. The LEs of the above circuit are calculated as follows:

$\lambda_1 = 4.0407$, $\lambda_2 = -0.13648$, $\lambda_3 = -0.274730$, $\lambda_4 = -0.28031$, and $\lambda_5 = -3.6701$

The LE as a function of time is shown in Figure 7.

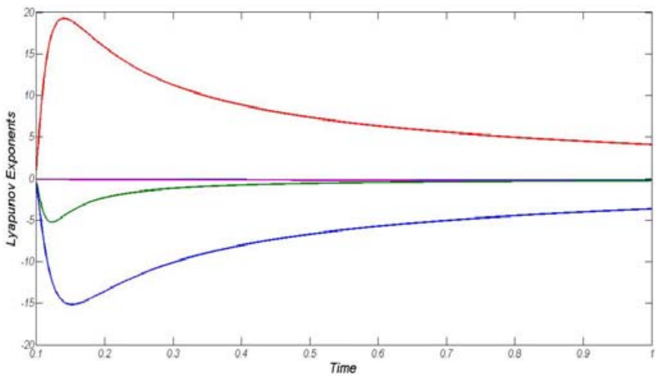

Fig. 7. Lyapunov exponents as a function of time.

5. NUMERIC SIMULATION AND CIRCUIT SIMULATION

For more explicitness and to conduct further investigations to verify the above analysis, a numeric simulation and a circuit simulation, respectively, using ADS and MATLAB is performed. Based on the analyses made above, that the system is a chaotic one.

5.1. Numeric Simulation

Simulation results indicate that the circuit has a chaotic behavior. Limit cycles for different initial conditions are shown in Figure 8.

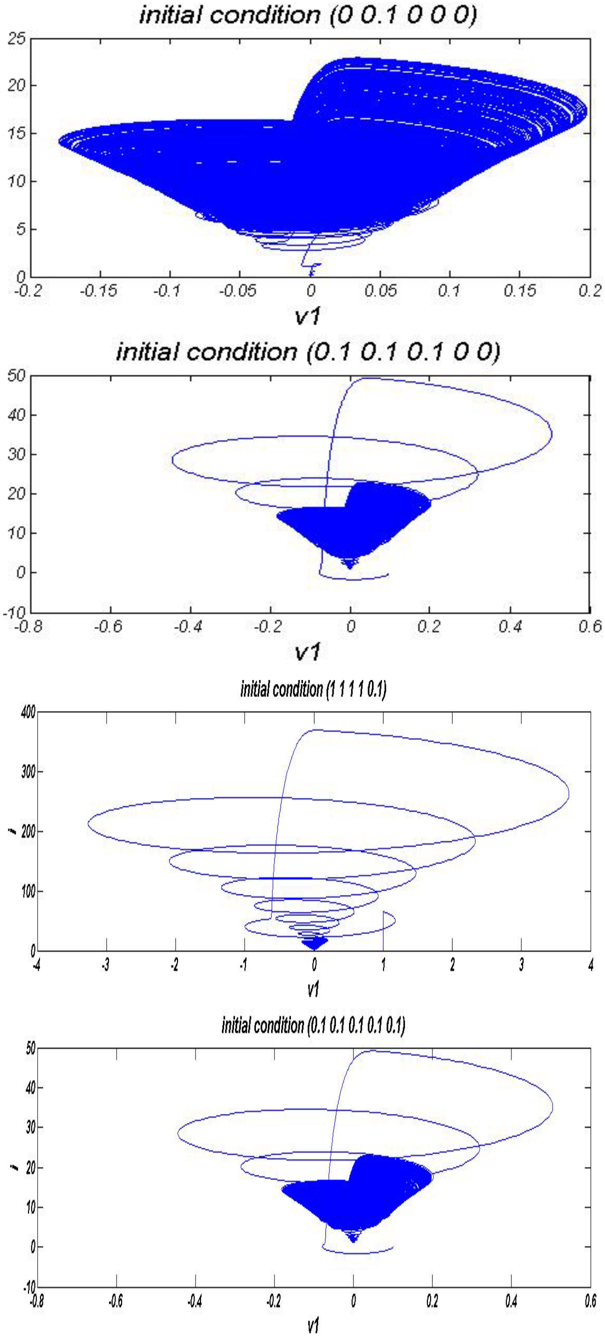

Fig. 8. Transient chaotic attractor in different initial conditions.

The chaotic attractor can be obtained from system (3), as depicted in Figure 9.

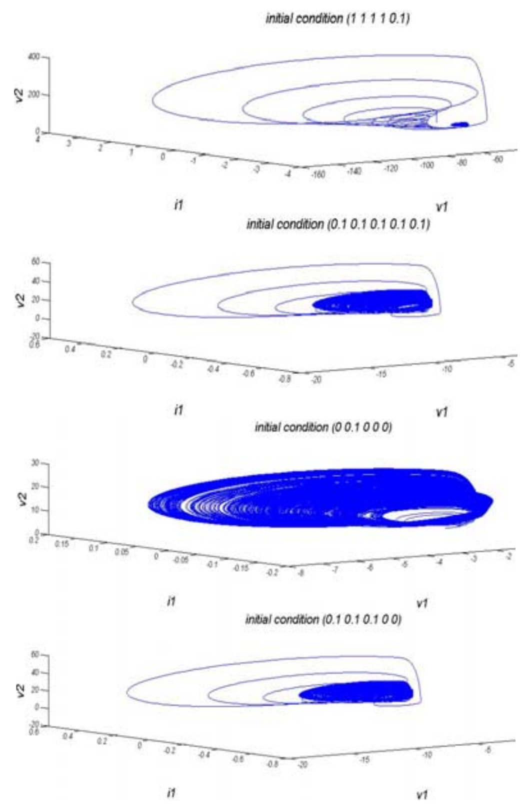

Fig. 9. 3D chaotic attractor in different initial condition.

5.2. Circuit Simulation Using ADS

With the aid of the proposed emulator, ADS software simulation experiments are conducted on the present chaotic circuit. The simulation results, shown in Figure 10. As shown in Figure 8, the attractor's figure is basically agreeable to the results of the numeric simulation.

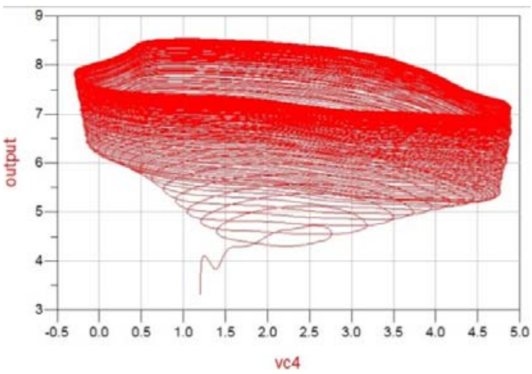

Fig. 10. Simulation results of projection onto $output - V_{c4}$.

6. POWER DENSITY SPECTRUM ANALYSIS OF THE CHAOTIC SYSTEM

An effective tool in the study of chaotic behavior is the frequency domain periodic analysis. In periodic signals, the energy is focused on some special frequencies, while in the chaotic behavior; the energy in different frequency values is non-zero. Therefore chaotic signals are wideband signals. In deterministic systems, a spectrum having a wideband represents the sign of starting a chaotic behavior (Boashash, 2003). Figure 11 shows the self-power density spectrum of the above circuit.

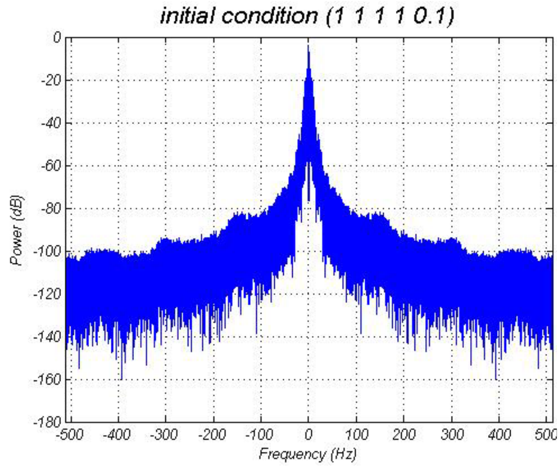

Fig.11. the self-power density spectrum chart of the chaotic oscillator

7. ENERGY DISTRIBUTION BASED ON THE DISCRETE WAVELET TRANSFORM

The Fourier transform of continuous signal in time $x(t)$ is obtained as follows:

$$X(f) = \int_{-\infty}^{\infty} x(t)\, e^{-j2\pi ft}\, dt$$

(12)

Where, t is the time and f the frequency; the Fourier transform gives us the spectral content of the signal, but in terms of time, it only attends to the whole signal during the time and does not focus on the time domain.

In order to enter time information in addition to signal frequency specifications, the short-time Fourier transform can be applied. The signal short-time Fourier transform $x(t)$ using a time window $w(t)$ is defined as follows:

$$STFT_x^w(\tau, f) = \int_{-\infty}^{\infty} x(t)\, w^*(t-\tau)\, e^{-j2\pi ft}\, dt \qquad (13)$$

where f is as a frequency variable and τ as a time variable; in the short-time Fourier transform, we do not know exactly what frequency component is available in the signal; rather, we will have only one range (a frequency band).

Wavelet Transform provides time-frequency information simultaneously that this is the advantage of Wavelet Transform over the short-time Fourier transform overcome the resolution problem of the short-time Fourier transform.

Signal frequency bands can be achieved using Wavelet Transform; therefore, the DWT can be used to obtain additional features of the signal. In contrast, the DWT is much easier than continuous wavelet transform. In the DWT for signal analysis, filters with different cut-off frequencies are used in different scales. For example, the signal is passed through low-pass and high-pass filters respectively to analyse low and high frequencies.

In DWT method the signal can be decomposed into different frequency bands. In this method two sets of coefficients are computed: approximation coefficients, and detail coefficients. The approximation coefficients are obtained by convolving the signal with the low-pass filter and detail coefficients are obtained by convolving the signal with the high-pass filter for detail.

Scaling as a mathematical operator shrinks or expands the signal. Thus, in high scales that the signal is expanded, we will have details; and in low scales that the signal is shrunk, we will have generality (Boashash, 2003).

It is well known that DWT is used for digitized (or sampled) signals to show their time-scale representation. In order to perform this transformation the original signal is passed through a band-pass filter (called by *G* and is named *mother wavelet*) to give a detail component for the first level. At the same level, convolving the signal with a low-pass filter (called by *H*) brings another component named approximate due to its low resolution. *G* and *H* are orthogonal vectors with $N \times 1$ elements (Boashash, 2003). For the second level, the approximate component is down-sampled by two, i.e. its samples are halved, and it is then passed through *G* and *H* to give detail and approximate components respectively at this level. Continuing this procedure up to the j^{th} level causes the original signal to be decomposed to *j* detail components and an approximate one. This procedure is shown in Figure 12 up to three decomposition levels for on-line applications. This new filter is well suited for on-line *1D* applications of wavelet transform, as the number of mathematical operations through its application is reduced (Volkovskii et al., 2005; Qin et al., 2011).

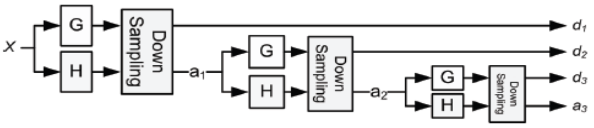

Fig. 12. Decomposition of original signal X by DWT up to three levels for online application.

As shown in Figure 13, this filtering process breaks the signal into multiple signals in which each new signal is determined by its coefficients, and each one belongs to a frequency band. In overall, discrete wavelet transform coefficients are divided into two categories of approximation coefficients and detail coefficients. Consider the signal $x(t)$, it can be decomposed in accordance to the discrete wavelet transform as follows:

$$A_{j+1}x(t) = \sum_{k\epsilon Z} c_{j,k}\varphi_{j,k} + \sum_{k\epsilon Z} d_{j,k}\psi_{j,k} \tag{14}$$

where, $A_{j+1}x(t)$ is the low frequency approximation of signal $x(t)$ with a scale coefficient $2^{-(j+1)}$, $\varphi(t)$ is the scale function and $\psi(t)$ is a mother wavelet function defined as

$$\psi_{j,k}(t) = \left\{ 2^{\left(\frac{j}{2}\right)}\Psi\left(2^{j}t-k\right), (j,k) \in Z \times Z \right\} \tag{15}$$

Also, $c_{j,k}$ is the general signal coefficient and $d_{j,k}$ is the coefficient of signal details computed as follows (Qin et al., 2011; Jiang et al., 2006).

$$\begin{aligned} c_{j,k} &= \sum_{m\epsilon Z} h^{*}_{m-2k} c_{j+1,m} \\ d_{j,k} &= \sum_{m\epsilon Z} g^{*}_{m-2k} d_{j+1,m} \end{aligned} \tag{16}$$

where, h_n are the low-pass filter coefficients and g_n are the high-pass filter coefficients.

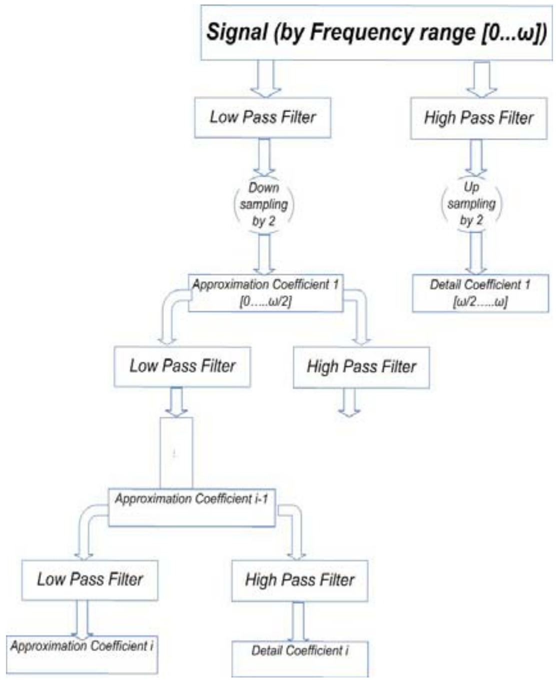

Fig. 13. The block diagram of signal decomposition by DWT.

The SWT provides efficient numerical solutions in the signal processing applications. It was independently developed by several researchers and under different names, e.g. the undecimated wavelet transform, the invariant wavelet transform and the redundant wavelet transform.

For a p-level decomposition, the highest frequency observed in the approximation wavelet coefficients c_j can be calculated as a function of the highest frequency observed sample frequency f_s as:

$$f_L = \frac{f_s}{2^{p+1}} \tag{17}$$

The frequency content of the approximation frequency band c_j and detail frequency bands d_j can be calculated as:

$$\begin{aligned} f_{c_j} &= \left[0, \frac{f_s}{2^{p+1}}\right] \\ f_{d_j} &= \left[\frac{f_s}{2^{p+1}}, \frac{f_s}{2^{p}}\right] \end{aligned} \tag{18}$$

The success of certain decomposition depends strongly on the chosen wavelet filters, depending on the signal properties

(Boashash, 2003). This is not the case with the STFT. Furthermore it is not possible to determine a mean value of a signal using the WT. In order to analyze more precisely, details and generalities of the signal can be extracted considering the DWT. By extracting the coefficient of the signal details using the wavelet transform, energy can be calculated for any detail coefficients as follows:

$$E(d_i) = \sum_{i=1}^{i=m} |d_i|^2 \qquad (16)$$

Where d_i is the details coefficients of level i, and the total energy can be calculated as follows:

$$E = \sum_{i=1}^{i=m} E(d_i) \qquad (17)$$

The growth rate of energy for each detail is calculated as follows:

$$\eta_i = \frac{E(d_i)}{E} \times 100 \qquad (18)$$

The algorithm is summarized as follows.

Step 1. Calculate of the DWT detail coefficient.
Step 2. Calculate the energy signal using the detailed coefficients.
Step 3. Determine the current state of the Energy distribution in different frequency level.

To illustrate irregular energy distribution of the signal details in each step, entropy is applied. Entropy is the irregularity degree in a system with energy or data. The less is a system regular, the more is the entropy. It is obvious that chaos is a wideband signal. In other words, it can be said that the energy distribution of signal details includes irregular changes in chaos signal (Boashash, 2003). Figure 13 shows distribution of the energy of signal details in each level in chaotic signal under different initial conditions.

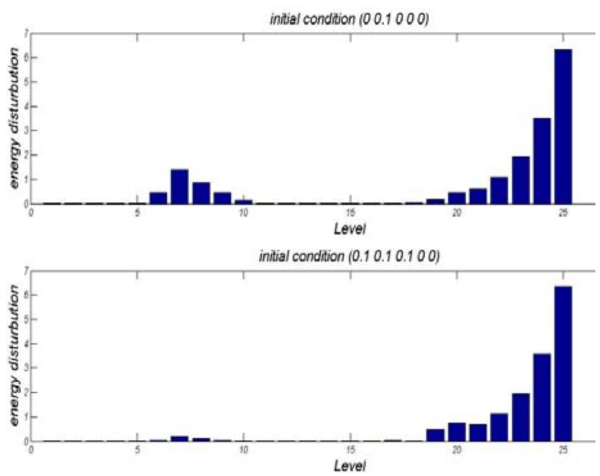

Fig. 13. Energy distribution using DWT.

7. CONCLUSIONS

In this paper, the dynamic of the new chaotic voltage control oscillator has been proposed based on Colpitts oscillators. The main aim of this paper is to analyze the chaotic voltage control oscillators stability and the chaos behavior under the theoretical and the numerical methods. The numerical simulation has been conducted by using ADS and MATLAB. For a nonlinear analysis of the chaotic circuit, the Lyapounov exponent method and the energy distribution based on multi resolution wavelet are deployed.

REFERENCES

Boashash, B., (2003). Time frequency Signal Analysis and Applications. *Control and Dynamic Systems,* vol. 78, pp.169.

Effa, J. Essimbi, B. Mucho, N. J. (2009). Synchronization of improved chaotic Colpitts oscillators using nonlinear feedback control. *J. Nonlinear Dyn.,* vol. 58, pp. 39–47.

Effa, J. Essimbi, B. Mucho, N. J. (2009). Synchronization of Colpitts oscillators with different orders. *Journal of Commun. Nonlinear Sci. Numer. Simulat.,* vol. 14, pp. 1590–1597.

Jiang, W. L., (2006). Orthogonal Wavelet Packet Analysis Based Chaos Recognition Method *Front. Electr. Electron. Eng. China*, Vol. 1, pp. 13-19.

Kengne, J. Chedjou, J.C. Kenne, G. Kyamakya, K. (2011). Dynamical properties and chaos synchronization of improved Colpitts oscillators. *Journal of Commun. Nonlinear Sci. Numer. Simulat.*, vol. 17, pp. 2914–2923.

Kennedy, M. P. (1994). Chaos in the Colpitts oscillator. *IEEE Trans. Circuits and Systems*, *vol. 41, pp. 771–774.*

Knop, W. Lauterborn, W. (1990). Bifurcation structure of in a damped driven Morse oscillator: A classical approach. *J. Chem. Phys*, vol. 86, pp. 5486–5493.

Lie, CG. Yuan, JM. (1986). Bistable and chaotic behavior in a damped driven Morse oscillator: A classical approach. J. Chem. Phys, vol. 86, pp. 5486–5493.

Qin Zhu, Shan, L., (2011). A Method for Detecting Chaotic Vibration Based on Continuous Wavelet Transform *Int. J. Sensing, Computing & Control*, Vol. 1, No. 2, pp. 125-132.

Shi, Z. Tong, J. H. (2010). A 3D chaotic oscillator's stability and chaos behavior. *IEEE International Workshop on Chaos-Fractal Theory and its Applications,* vol. 31, pp. 207 210.

Tama, A. Namajunas, A. and Cenys, A. (1996). Simple 4D chaotic oscillator. *Electronics Letters*, vol. 32(II), pp. 957–958.

Volkovskii, A. R. Tsimring, L. S. Rulkov, N. F. Langmore, (2005). Spread spectrum communication system with chaotic frequency modulation. American Institute of Physics, (Chaos), vol. 15, pp. 033101-1-6.

Zhu, Q. Liang, S. (2011). A Method for Detecting Vibration Based on Continuous Wavelet Transform. *Int. J. Sensing Computing & Control*, vol. 1, No. 2, pp. 125–132.